Electronic Supporting Information

Mechanistic insights into copper-catalyzed aerobic oxidative coupling of N–N bonds

*Michael C. Ryan,[a] Yeon Jung Kim,[a] James B. Gerken,[a] Fei Wang,[a] Michael M. Aristov,[a] Joseph R. Martinelli,[b] and Shannon S. Stahl[a]**

[a]*Department of Chemistry, University of Wisconsin-Madison, 1101 University Avenue, Madison, Wisconsin 53706, United States*
[b]*Small Molecule Design and Development, Lilly Research Laboratories, Eli Lilly and Company, Indianapolis, Indiana 46285, United States*

stahl@chem.wisc.edu

Table of Contents

1. General considerations

All commercially available reagents were purchased from Sigma-Aldrich and used as received, except where otherwise noted. All *para*-substituted N–H imines were prepared according to literature procedure.[1] ^{1}H, ^{13}C, and ^{19}F NMR spectra were recorded on a Bruker Avance III 400 spectrometer (^{1}H 400.1 MHz, ^{13}C 100.6 MHz, ^{19}F 376.5 MHz) or a Bruker Avance III 500 spectrometer (^{1}H 500.1 MHz, ^{13}C 125.7 MHz, ^{19}F 470.6 MHz) and chemical shifts are reported in parts per million (ppm). NMR spectra were referenced to $CDCl_3$ at 7.26 ppm (^{1}H) and 77.16 ppm (^{13}C), and or d^6-DMSO at 2.50 ppm (^{1}H) and 39.52 ppm (^{13}C). All ^{19}F NMR spectra were absolutely referenced to their respective solvent peaks in the ^{1}H NMR spectrum. Chromatography was performed using an automated Biotage Isolera® or Teledyne Isco Combiflash Rf with reusable 25 g Redisep Rf cartridges hand packed with standard silica or Biotage® SNAP Ultra C18 60 g prepacked cartridges. UV−visible spectra were acquired using an Agilent Cary 60 spectrometer. Cyclic voltammetry measurements were performed using a BASi Epsilon potentiostat. HPLC analysis was performed on a Shimatzu Prominence HPLC system.

Note – caution should be used when conducting reactions in organic solvents using oxygen gas. Efforts should be made to stay below the limiting oxygen concentration (LOC) of the solvent and/or reagents used in the reaction. For information about the LOC of industrially relevant solvents, see Reference 2.

2. Synthesis of imidoyl amidine 1

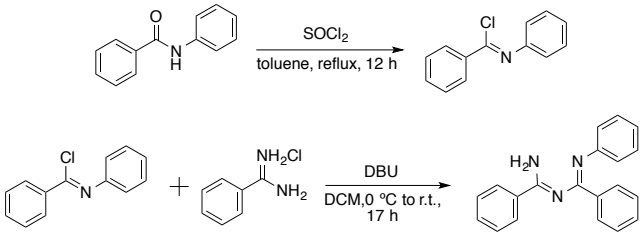

In a procedure adapted from the literature,[3] N-phenylbenzamide (20 g, 101 mmol, 1 equiv) and toluene (63 mL) were added to a three-neck round bottom flask with reflux condenser and stir bar and placed under N_2 atmosphere. Thionyl chloride (36 mL, 505 mmol, 5 equiv) was added via syringe. The reaction mixture was stirred at reflux for 12 h. The reaction was cooled to room temperature and the solvent and thionyl chloride was removed in vacuo. Sodium hydrogen carbonate was added and diluted with DCM. Solids were removed via filtration, and then the solvent was removed in vacuo to yield the desired imidoyl amidine in quantitative yield. The imidoyl amidine was used for the next reaction without further purification.

A 100 mL round bottom flask with stir bar was charged with benzamidine hydrochloride (2.18 g, 13.9 mmol, 1 equiv), DCM (23 mL), and DBU (4.15 mL, 27.8 mmol, 2 equiv). The solution was cooled to 0 degrees with an ice/water bath. Iminoyl chloride (3 g, 13.9 mmol, 1 equiv) was dissolved in 23 mL of DCM and added slowly dropwise over 10 minutes. After 10 minutes, the reaction was warmed to room temperature and allowed to stir for 17 hours. After 17 hours, the reaction was quenched with saturated aqueous sodium bicarbonate (50 mL). The layers were shaken and separated. The aqueous phase was extracted with DCM (2x 50 mL each). The combined organics were washed with water (50 mL), dried over sodium sulfate, filtered, and concentrated. The crude product was purified via silica gel chromatography (9:1 to 1:1 pentane:EtOAc) to yield **1** as an off-white solid (7.08 mmol, 51% yield). ^{1}H NMR (MeOH-d_4) δ 8.13 – 7.90 (m, 2H), 7.67 – 7.55 (m, 2H), 7.52 – 7.44 (m, 4H), 7.39 (t, J = 7.6 Hz, 2H), 7.27 (t, J = 7.7 Hz, 2H), 7.14 – 7.01 (m, 3H). Remaining spectral data matches previously reported values.[4]

3. Catalytic synthesis of triazole 2 (Figure 1A)

A vial with stir bar was charged with imidoylamidine 1 (60 mg, 0.2 mmol) and CuBr•DMS (4.1 mg, 0.02 mmol) and fitted with a septum. The vials were purged with O_2. DMSO (1 mL) was added via syringe. These reactions were heated to 80 ºC for 17 h. After 17 h, the reaction was cooled to room temperature, diluted with ether (10 mL), and washed 3 times with water (10 mL). The organic phase was concentrated in vacuo, 1,1,2,2-tetrachloroethane (0.1 mmol) was added as an internal standard, and the crude reaction mixture was dissolved in $CDCl_3$. The yield of triazole 2 was determined by ^1H NMR.

4. Kinetic studies of triazole formation (Figure 1B)

HPLC calibration curve of triazole 2

Stock solutions of benzophenone internal standard were prepared via serial dilution: 5 mM benzophenone (23 mg in 25 mL EtOAc, 0.125 mmol) was made, then 2.5 mL of this solution was diluted to 25 mL to generate a 0.5 mM benzophenone solution. Stock solutions of triazole **2** were prepared via serial dilution: 3.36 mM triazole **2** in EtOAc (25 mg, 0.11 mmol, in 25 mL) was made, then 3.72 mL was diluted to 25 mL to generate a 0.5 mM **2** solution. Different ratios of the 0.5 mM solutions were transferred to HPLC vials to generate solutions that totaled to 1 mL:

Vol 0.5 mM Benzophenone (mL)	Vol 0.5 mM **2** (mL)	[triazole]/[benzophenone]
0.5	0.5	1
0.33	0.67	2
0.25	0.75	3
0.2	0.8	4
0.17	0.83	5
0.14	0.86	6

Each solution was analyzed by HPLC, and the relative integrals of the triazole and benzophenone curves were obtained to generate the calibration curve below (Figure S1). HPLC conditions: 70/30 MeCN/H_2O containing 0.1% formic acid, 1 mL/min, C18 column, 254 nm, r.t.; (triazole)=5.17 min, r.t.(benzophenone)=3.69 min.

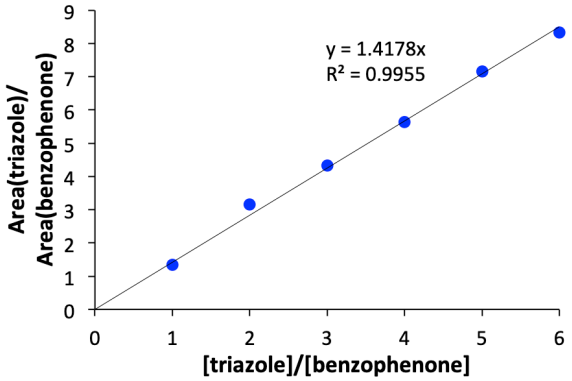

Figure S1. HPLC calibration curve of triazole **2** using benzophenone as an internal standard.

Imidoylamidine oxidation time course – Cu dependence

A vial with stir bar was charged with **1** (0.27 mmol) and fitted with a septum. The vial was fitted with an O_2 balloon and the headspace was purged. Two stock solutions were made: 1) 100 mM CuBr•DMS and 20 mM benzophenone (internal standard) in DMSO and 2) 20 mM benzophenone in DMSO. Different ratios of these stock solutions were added to the vial, depending on the desired [Cu]. For example, for the 50 mM Cu reaction, 0.5 mL of the blank benzophenone solution was added to the vial containing **1**. The vial was placed in an aluminum block pre-heated to 80 ºC and allowed to equilibrate for 15 min. After 15 min, 0.5 mL of the Cu solution was added. Aliquots (25 µL) of the reaction were periodically removed and diluted with EtOAc. The reaction was monitored by reverse phase HPLC (70/30 MeCN/H_2O containing 1% formic acid) and the [**2**] at each timepoint was determined via relative integration to the benzophenone internal standard. The data points were plotted and fitted with a linear regression to determine the initial rates d[triazole]/dt (mM/min) (Figure S2). The initial rates were then plotted against [CuBr•DMS] to determine that the reaction is second order in CuBr•DMS (Figure 1B in the manuscript).

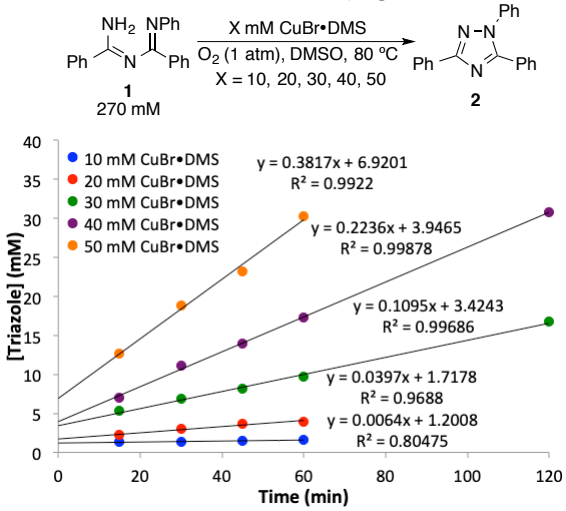

Figure S2. Initial rates of N–N bond formation of triazole **2** varying [CuBr•DMS].

Imidoylamidine oxidation time course – O_2 Dependence

O_2 Dependence (0.06, 0.21 atm, 1 atm). A vial with stir bar was charged with **1** (0.27 mmol) and fitted with a septum. The vial was fitted with either a balloon containing either pure O_2 (1 atm), air (0.21 atm), or a balloon containing 6% O_2 in N_2 (0.06 atm). The headspace was purged. A stock solution of 40 mM CuBr•DMS and 40 mM benzophenone in DMSO (1 mmol of each component in 25 mL) was made. This solution (1 mL) was added to the vials which were placed in an aluminum block pre-heated to 80 ºC. Aliquots (25 µL) of the reaction were removed periodically and diluted with EtOAc. The reaction was monitored by reverse phase HPLC (70/30 MeCN/H_2O containing 1% formic acid), and the [**2**] at each timepoint was determined via relative integration to the benzophenone internal standard. The data points were plotted and fitted with a linear regression to determine the initial rates d[triazole]/dt (mM/min) (Figure S4). The initial rates were then plotted against P_{O2} (atm) and fitted to a linear regression to determine that the reaction is first order in O_2 (Figure 1 in the manuscript).

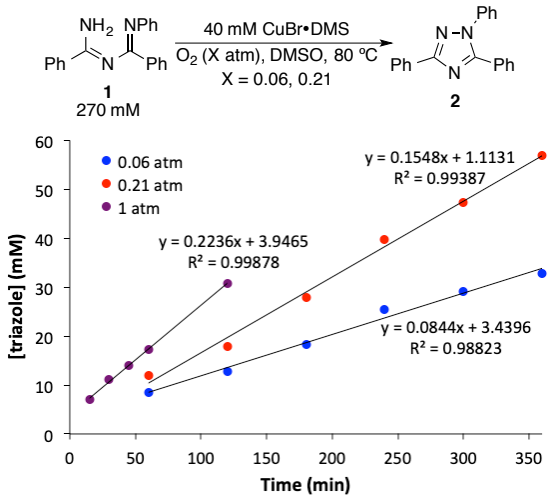

Figure S3. Initial rates of N–N bond formation of triazole **2** varying P_{O2}

O_2 dependence (1.5, 1.75 atm). A heavy-walled tube with stir bar was charged with **1** (0.27 mmol). This tube was attached to a pressure transducer, evacuated and refilled with 1 atm O_2 three times, and then pressurized to the appropriate pressure. The tube was placed in an 80 ºC bath. Meanwhile, a stock solution of 40 mM CuBr•DMS in DMSO (1 mmol in 25 mL) was made. 1 mL of this copper solution was added to the tube and the pressure was monitored. The data points were plotted and fitted with a linear regression to determine the rate of O_2 consumption (Figure S5). To convert O_2 uptake data to d[triazole]/dt (mM/min) for Figure 1, the slope was multiplied by 2 (2 equiv triazole made for every 1 equiv O_2). The initial rates were then plotted against P_{O2} (atm) and fitted to a linear regression to determine that the reaction is first order in O_2 (Figure 1 in the manuscript).

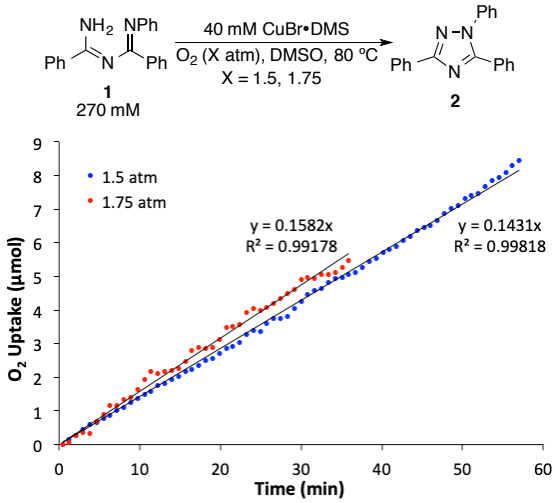

Figure S4. Initial rates of N–N bond formation of triazole **2** varying P_{O2} at >1 atm.

Imidoylamidine oxidation time course – substrate dependence

A vial with stir bar was charged with **1** (0.2, 0.4, and 0.5 mmol depending on the concentration of desired **1**) and fitted with a septum. The vial was fitted with an O_2 balloon and the headspace was purged. A stock solution of 40 mM CuBr•DMS and 40 mM benzophenone in DMSO (1 mmol of each component in 25 mL) was made. This solution (1 mL) was added to the vials which were placed in an aluminum block pre-heated to 80 ºC. Aliquots (25 µL) of the reaction were removed periodically and diluted with EtOAc. The reaction was monitored by reverse phase HPLC (70/30 MeCN/H_2O containing 1% formic acid) and the [**2**] at each timepoint was determined via relative integration to the benzophenone internal standard. The data points were plotted and fitted with a linear regression to determine the initial rates d[triazole]/dt (mM/min) (Figure S3). The initial rates were then plotted against [**1**] to determine that the reaction is inhibited by substrate (Figure 1B in the manuscript).

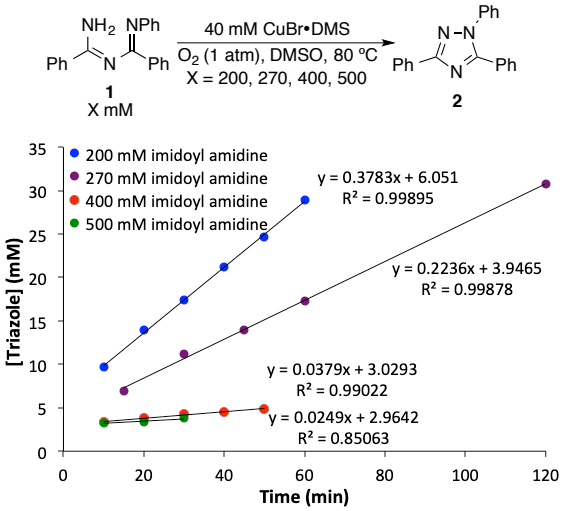

Figure S5. Initial rates of N–N bond formation of triazole **2** varying [**1**].

5. Catalyst optimization studies of benzophenone imine N–N coupling (Figure 2A)

A test tube was charged with 4,4′-difluorobenzophenone azine **3** (43 mg, 0.2 mmol, 1 equiv.), ligand (0.04-0.08 mmol, 0.2-0.4 eq.), and a copper source (0.04 mmol, 0.2 eq.). 1 mL of solvent was added and the tubes were placed in a parallel orbital-mixing shaker reactor. The headspace of the test tube was purged three times with O_2, sealed with an O_2 pressure slightly above 1 atm, and the reaction was stirred for 5 h. After 5 h, the reactions were cooled to room temperature and concentrated *in vacuo*. 4,4′-difluorobiphenyl (3.8 mg, 0.1 mmol) was then added as an internal standard for quantitative NMR analysis. The reaction mixture was dissolved in $CDCl_3$ and yields were determined by ^{19}F NMR.

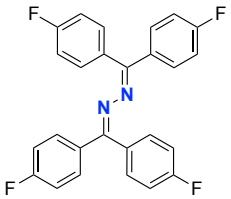

^1H NMR (400 MHz, $CDCl_3$) δ 7.53 – 7.42 (m, 4H), 7.37 – 7.29 (m, 4H), 7.13 (t, J = 8.7 Hz, 4H), 7.00 (t, J = 8.7 Hz, 4H). ^{13}C NMR (100 MHz, $CDCl_3$) δ 163.9 (d, J = 250.9 Hz), 162.8 (d, J = 249.4 Hz), 158.8, 134.0 (d, J = 3.1 Hz), 131.4 (d, J = 8.2 Hz), 131.1 (d, J = 3.5 Hz), 130.6 (d, J = 8.5 Hz), 115.2 (d, J = 21.7 Hz), 115.1 (d, J = 21.6 Hz). ^{19}F NMR (377 MHz, $CDCl_3$) δ -110.44 (s), -111.22 (s).
HRMS (**ESI**) Calculated for $[M+H]^+$: 433.1322, measured: 433.1318.

A. Table S1 -Ligand screen

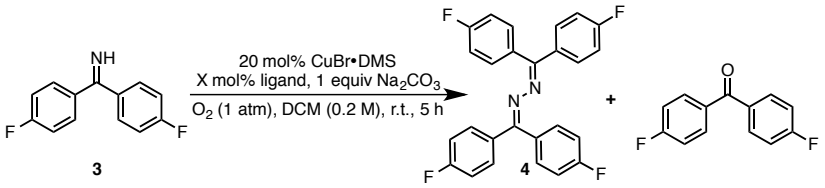

entry	ligand	X	Mass Balance (%)	conversion (%)	benzophenone (%)	yield (%)[a]
1	**none**	**N/A**	**97**	**40**	**10**	**27**
2	**pyridine**	**40**	**98.5**	**37.5**	**9**	**27**
3	4-MeO-pyridine	40	101	27	9	19
4	DMAP	40	97	28	9	19
5	NMI	40	99.5	15	8.5	6
6	1,10-phenanthroline	20	104	4	8	0
7	bpy	20	104	4.5	7.5	1
8	MeO-bpy	20	100.5	10	8.5	2
9	TMEDA	20	101.5	15	8.5	8
10	NMI/bpy	40/20	102	6	8	0

[a] Yields determined by ^{19}F NMR by integration relative to 4,4'-difluorobiphenyl internal standard.

B. Table S2 - Solvent screen

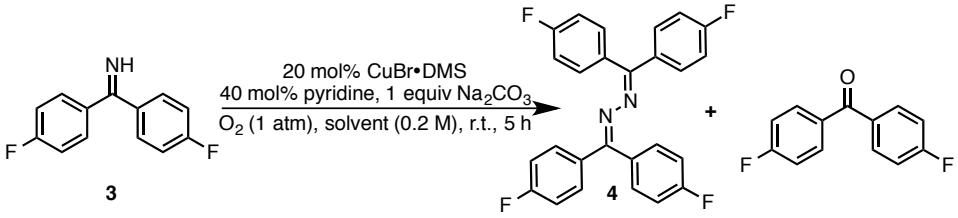

entry	Solvent	Mass Balance (%)	conversion (%)	benzophenone (%)	yield (%)[a]
1	toluene	91	20	8	3
2	**DMF**	**103**	**84**	**5**	**82**
3	MeCN	69.5	51	8	13
4	THF	102	39	8	34
5	DMSO	107	71	10	68
6	EtOAc	73	42	7	8
7	Acetone	89	44	7	26
8	NMP	97.5	42.5	8	32
9	DME	102.5	30.5	8	25
10	$MeNO_2$	70	42	9	3

[a] Yields determined by ^{19}F NMR by integration relative to 4,4'-difluorobiphenyl internal standard.

C. Table S3 – Cu source screen

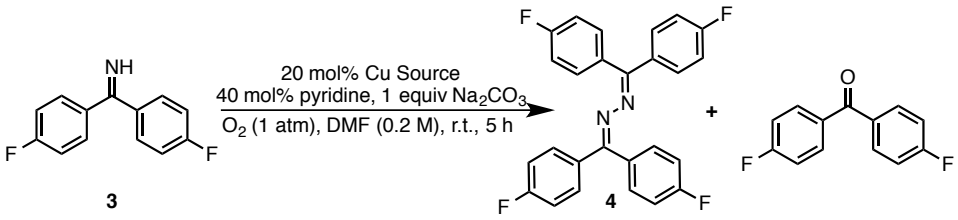

entry	Cu Source	Mass Balance (%)	conversion (%)	benzophenone (%)	yield (%)[a]
1	CuBr*DMS	**103**	**84**	**5**	**82**
2	CuI	101.5	34.5	4	32
3	$Cu(MeCN)_4PF_6$	100	4	4	0
4	CuCl	100	61	4	57
5	CuTc	100	13	4	9
6	$Cu(OAc)_2$	99.5	5	4.5	0
7	$CuCl_2$	103	26	4	25
8	$CuBr_2$	96.5	76.5	3	70
9	$Cu(NO_3)_2•H_2O$	98.5	12.5	5	6
10	$Cu(BF_4)_2•H_2O$	98.5	7.5	5	1

[a] Yields determined by ^{19}F NMR by integration relative to 4,4'-difluorobiphenyl internal standard.

D. Table S4 - Additive screen

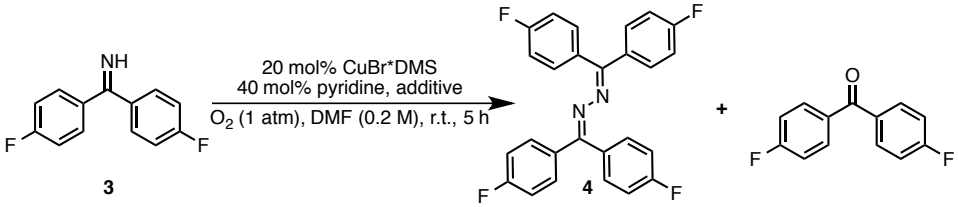

entry	additive	Mass Balance (%)	conversion (%)	benzophenone (%)	yield (%)[a]
1	**None**	**103**	**89.5**	**4.5**	**88**
2	1 equiv NaOH	98	14	6	6
3	1 equiv K_3PO_4	95.5	86.5	4	78
4	1 equiv $NaHCO_3$	97	82	4	75
5	1 equiv KO*t*Bu	74	32	6	0
6	1 equiv Ag_2CO_3	97	68	4	61
7	1 equiv NH_4OAc	93.5	16.5	10	0
8	20 mol% TEMPO + 1 equiv Na_2CO_3	98.5	88.5	4	83
9	20 mol% Bu_4NBr + 1 equiv Na_2CO_3	96	57.5	4.5	49
10	1 eq. Bu_4NBr + 1equiv Na_2CO_3	101	16.5	4.5	13

[a] Yields determined by ^{19}F NMR by integration relative to 4,4'-difluorobiphenyl internal standard.

6. Kinetic studies of azine formation (Figure 2B)

N–H imine oxidation time course – Cu dependence

A vial with stir bar was charged with imine **3** (217 mg, 1 mmol) and 4,4′-difluorobiphenyl (internal standard) (19 mg, 0.1 mmol) and fitted with a septum. An O_2 balloon was fitted to the top of the vial and the headspace was purged with oxygen. DMF was added to the vial (see table below for amount) to dissolve the substrate and this solution was heated to 40 ºC in an aluminum heating block. A stock solution of CuBr•DMS and pyridine in DMF (100 mM in Cu, 200 mM in pyridine) was prepared. The desired volume of the Cu solution was added to the substrate vial, and then aliquots (~0.1 mL) were periodically removed from the reaction and added to NMR tubes containing $CDCl_3$. Reaction progress was monitored by ^{19}F NMR spectroscopy by integration of the product diazine **4** relative to internal standard. The data points were plotted and fitted with a linear regression to determine the initial rates d[azine]/dt (mM/min) (Figure S6). The initial rates were then plotted against $[(pyr)_2CuBr]$ to determine that the reaction is second order in [Cu] (Figure 2B in the manuscript).

Entry	Volume DMF (mL)	V 100 mM CuBr•DMS and 200 mM pyridine stock solution (mL)	Final [Cu] mM
1	4.75	0.25	40
2	4.5	0.5	20
3	4.25	0.75	15
4	4	1	10
5	3	2	5

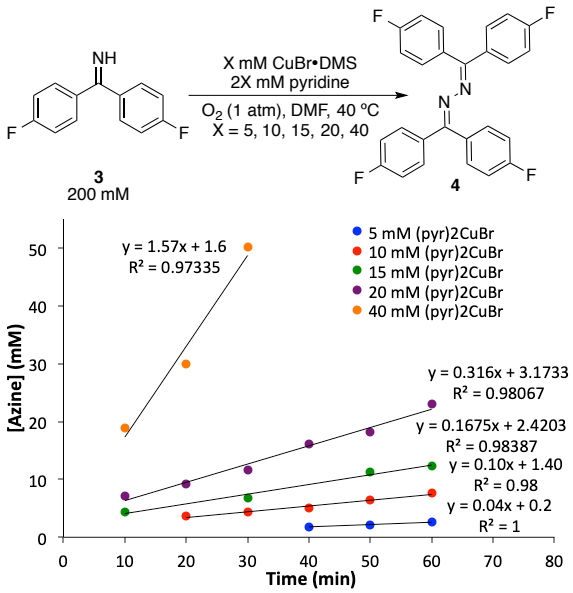

Figure S6. Initial rates of N–N bond formation of azine **4** varying [(pyr)2CuBr].

N–H imine oxidation time course – O_2 dependence

O_2 Dependence (0.09, 0.21, 1 atm). A vial with stir bar was charged with imine **3** (217 mg, 1 mmol) and 4,4′-difluorobiphenyl (internal standard) (19 mg, 0.1 mmol) and fitted with a septum. The vial was fitted with either a balloon containing either pure O_2 (1 atm), air (0.21 atm), or a balloon containing 6% O_2 in N_2 (0.09 atm) and the headspace was purged. DMF (4 mL) was added to the vial to dissolve the substrate and this solution was heated to 40 ºC in an aluminum heating block. A stock solution of CuBr•DMS and pyridine in DMF (100 mM in Cu, 200 mM in pyridine) was prepared. This Cu solution was added to the substrate vial (1 mL). Aliquots (~0.1 mL) were removed from the reaction and added to NMR tubes containing $CDCl_3$. Reaction progress was monitored by ^{19}F NMR spectroscopy by integration of **4** relative to internal standard. The data points were plotted and fitted with a linear regression to determine the initial rates d[azine]/dt (mM/min) (Figure S9). The initial rates were then plotted against P_{O2} (atm) and fitted to a linear regression to determine that the reaction is first order in O_2 (Figure 2B in the manuscript).

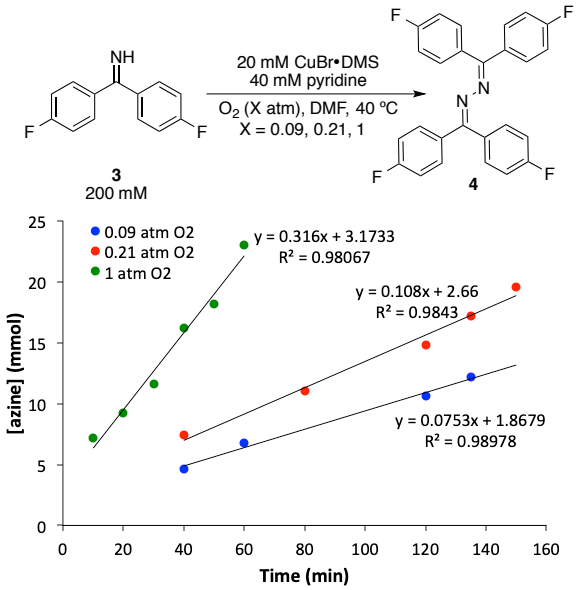

Figure S7. Initial rates of N–N bond formation of azine **4** varying P_{O2}.

O_2 dependence (1.5, 2 atm). A heavy walled tube with stir bar was charged with imine (43 mg, 0.2 mmol) and DMF (0.7 mL). This tube was attached to a pressure transducer, evacuated and refilled with 1 atm O_2 three times, and then pressurized to the appropriate pressure. The vial was placed in a 40 ºC oil bath. Meanwhile, a 66 mM solution of CuBr•DMS and 132 mM pyridine in DMF was prepared. 0.3 mL of this copper solution was added to the tube and the pressure was monitored. The data points were plotted and fitted with a linear regression to determine the rate of O_2 consumption (Figure S10). To convert O_2 uptake data to d[azine]/dt (mM/min) for Figure 3, the slope was multiplied by 2 (2 equiv azine made for every 1 equiv O_2). The initial rates were then plotted against P_{O2} (atm) and fitted to a linear regression to determine that the reaction is first order in O_2 (Figure 2B in the manuscript).

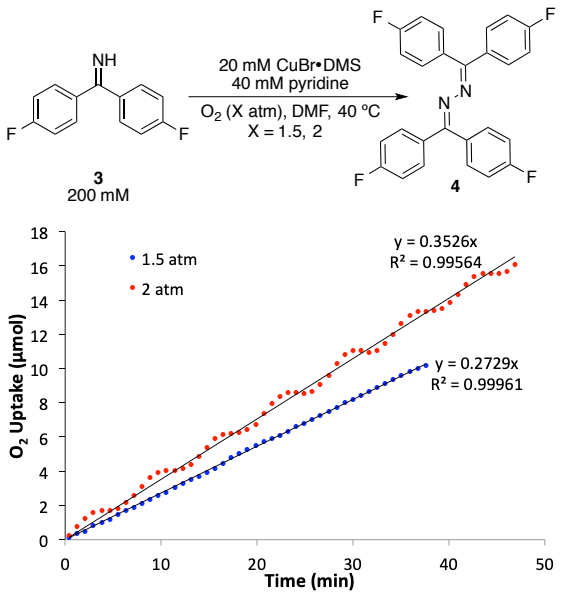

Figure S8. Initial rates of N–N bond formation of azine **4** varying P_{O2} at >1 atm.

N–H imine oxidation time course – substrate dependence

A vial with stir bar was charged with imine (0.25 - 2.5 mmol) and 4,4′-difluorobiphenyl (internal standard) (19 mg, 0.1 mmol) and fitted with a septum. An O_2 balloon was fitted to the top of the vial and the headspace was purged with oxygen. DMF (4 mL) was added to the vial to dissolve the substrate and this solution was heated to 40 ºC in an aluminum heating block. A stock solution of CuBr•DMS and pyridine in DMF (100 mM in Cu, 200 mM in pyridine) was prepared and then 1 mL of this Cu solution was added to the vial. Aliquots (~0.1 mL) were periodically removed from the reaction and added to NMR tubes containing $CDCl_3$. Reaction progress was monitored by ^{19}F NMR spectroscopy by integration of **4** relative to an internal standard. The data points were plotted and fitted with a linear regression to determine the initial rates d[azine]/dt (mM/min) (Figure S6). The initial rates were then plotted against [**3**] to determine that the reaction is inhibited by substrate (Figure 2B in the manuscript).

Entry	Quantity imine (mmol)	Final [imine] mM
1	0.25	50
2	0.5	100
3	0.75	150
4	1.5	300
5	2.5	500

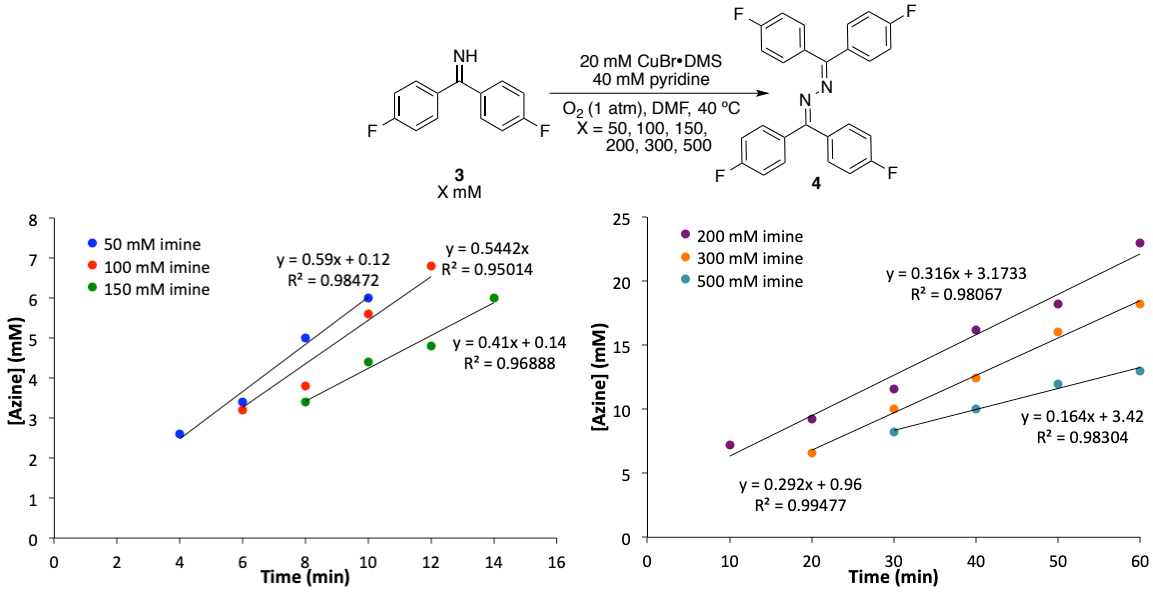

Figure S9. Initial rates of N–N bond formation of azine **4** varying [**3**] (50-150 mM, left, and 200-500 mM, right).

N–H imine oxidation time course – pyridine dependence

A vial with stir bar was charged with CuBr•DMS (21 mg, 0.1 mmol), pyridine in DMF (see table below), and DMF to a final volume of 3 mL. The vial was fitted with a septum and O_2, then the headspace was purged. The solution was heated to 40 ºC in an aluminum heating block. A stock solution of imine (1.09 g, 5 mmol) and internal standard (95 mg, 0.5 mmol) in DMF (10 mL) was made and added to each reaction (2 mL). Aliquots (~0.1 mL) were removed from the reaction and added to NMR tubes containing $CDCl_3$. Reaction progress was monitored by ^{19}F NMR spectroscopy by integration of **4** relative to an internal standard. The data points were plotted and fitted with a linear regression to determine the initial rates d[azine]/dt (mM/min) (Figure S8). The initial rates were then plotted against [pyridine] to determine that the reaction is first order in pyridine (Figure 2B in the manuscript).

Entry	Volume 2 M pyridine (mL)	Volume 0.5 M pyridine (mL)	Final [pyridine] mM
1	-	0	0
2	-	1	50
3	-	2	100
4	1	-	400
5	1.5	-	600

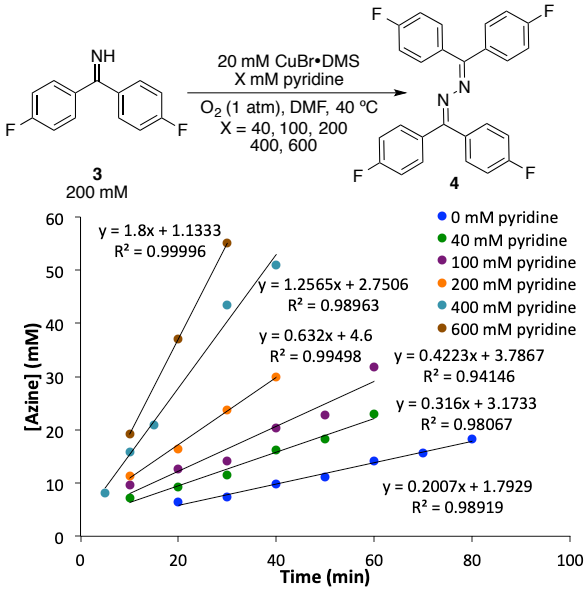

Figure S10. Initial rates of N–N bond formation of azine **4** varying [pyridine].

7. General procedures for cyclic voltammetry experiments (Figure 3)

All cyclic voltammetry (CV) measurements were conducted at room temperature. A three-electrode system with a glassy carbon working electrode (3 mm diameter), a Pt wire counter electrode, and an Ag/Ag^+ non-aqueous reference electrode were used at scan rate = 100 mV/s. The redox potentials of either ferrocenium/ferrocene ($Fc^{+/0}$) or decamethylferrocenium/decamethylferrocene ($Me_{10}Fe^{+/0}$) were measured as internal references, with the specific reference selected to avoid overlap with other redox processes. All measured potentials were referenced to $Fc^{+/0}$.[5] In N,N-dimethylformamide, $Me_{10}Fe^{+/0}$ is - 0.458 V vs $Fc^{+/0}$.[6] Due to complications arising from facile aerobic oxidation and/or disproportionation of Cu(I) in DMF, 1:1 $Cu(OTf)_2$ and Bu_4NBr was used in place of CuBr. The measurement conditions were $Cu(OTf)_2$ (5 mM), Bu_4NBr (5 mM), benzophenone imine (50 mM), and pyridine (1-60 equiv) in DMF (10 mL) with Bu_4NPF_6 (0.1 M) as the supporting electrolyte.

8. O_2 uptake of catalytic aerobic oxidation of 1 and 3 (Figure 4)

O_2 uptake of triazole formation reaction

A heavy-walled tube with stir bar was charged with imidoylamidine **1** (0.27 mmol). This tube was attached to a pressure transducer, evacuated and refilled with 1 atm O_2 three times, and then pressurized to 2 atm. The tube was placed in an 80 ºC bath. Meanwhile, a stock solution of 40 mM CuBr•DMS in DMSO (1 mmol in 25 mL) was made, then 1 mL of this copper solution was added to the tube and the pressure was monitored for 420 min.

O_2 uptake of azine formation reaction

A heavy-walled tube with stir bar was charged with a solution of imine **3** (0.20 mmol) in DMF (0.7 mL). This tube was attached to a pressure transducer, evacuated and refilled with 1 atm O_2 three times, and then pressurized to 2 atm. The tube was placed in an 40 ºC bath. Meanwhile, a stock solution of 66 mM CuBr•DMS and 132 mM pyridine in DMF (1.65 mmol CuBr•DMS and 3.3 mmol pyridine in 25 mL) was made, then 0.3 mL of this copper solution was added to the tube and the pressure was monitored for 420 min.

9. Procedures for stoichiometric anaerobic N–N coupling

Synthesis of Cu complexes [(imam)$CuCl_2$] and [$(imam)_2Cu](PF_6)_2$

[(imam)$CuCl_2$]: A vial with stir bar was charged with $CuCl_2$ (27 mg, 0.2 mmol, 1 equiv) and dissolved in EtOH (0.5 mL). Imidoyl amidine **1** (60 mg, 0.2 mmol, 1 equiv) was added in one portion and the reaction was allowed to stir for 30 minutes. A dark green precipitate formed upon addition of **1**. This precipitate was filtered, washed with ether (~20 mL), and dried in air. Quantitative yield (87 mg, 0.2 mmol, >99%) of (imam)$CuCl_2$ as a dark green solid. Dark green crystals of (imam)$CuCl_2$ were grown from MeOH/EtOH at -20 ºC over the course of 2 days. X-ray crystallography of these crystals indicates that complex unit cell parameters match those of the known complex.[4]

[$(imam)_2Cu](PF_6)_2$: Imidoyl amidine **1** (500 mg, 1.67 mmol, 2 equiv), $CuCl_2$•$2H_2O$ (142 mg, 0.84 mmol, 1 equiv), NH_4PF_6 (272 mg, 1.67 mmol, 2 equiv), and THF (17 mL) were added to a round bottom flask with stir bar and stirred for 4 hours. After 4 hours the reaction was filtered and washed with copious amounts of THF (500 mL). The green filtrate was concentrated to yield a purple solid. The solid as dissolved in MeCN, triturated with ether, and dried in vacuo to yield $(imam)_2Cu(PF_6)_2$ (231 mg, 0.24 mmol, 29% yield) as a purple solid. Dark purple crystals of $(imam)_2Cu(PF_6)_2$•$2Et_2O$ were obtained by slow diffusion of Et_2O into a solution of $(imam)_2Cu(PF_6)_2$ in MeCN.

Stoichiometric N–N coupling from [(imam)$CuCl_2$] (eq 1)

A vial with stir bar was brought into the glovebox and charged with a 50 mM solution of [(imam)$CuCl_2$] (66 mg, 0.15 mmol) and benzophenone (internal standard) (5.4 mg, 0.03 mmol) in degassed DMSO (3 mL). The vial was fitted with a septum, taken out of the glovebox, and heated to 80 ºC. After 5 min, an aliquot (25 µL) of the reaction was taken out and diluted with EtOAc. The reaction was monitored by reverse phase HPLC (70/30 MeCN/H_2O containing 1% formic acid), and a 33% yield of **2** was obtained relative to the total [(imam)$CuCl_2$] added. After 2 h, the same yield was obtained.

Stoichiometric N–N coupling from [(imam)$CuCl_2$] and benzamidine (eq 2)

A vial with stir bar was brought into the glovebox and charged with a 50 mM solution of (imam)$CuCl_2$ (66 mg, 0.15 mmol), benzamidine (18 mg, 0.15 mmol, 1 equiv), and benzophenone (internal standard) (5.4 mg, 0.03 mmol) in degassed DMSO (3 mL). The vial was fitted with a septum, taken out of the glovebox, and heated to 80 ºC. After 2 h, an aliquot (25 µL) of the reaction was taken out and diluted with EtOAc. The reaction was monitored by reverse phase HPLC (70/30 MeCN/H_2O containing 1% formic acid), and a 50% yield of **2** was obtained relative to the total [(imam)$CuCl_2$] added.

Stoichiometric N–N coupling from [(imam)$_2$Cu](PF$_6$)$_2$ (eq 3)

A vial with stir bar was brought into the glovebox and charged with a 20 mM solution of (imam)$_2$Cu(PF$_6$)$_2$ (67 mg, 0.07 mmol), benzophenone (internal standard) (12.6 mg, 0.07 mmol) in degassed DMSO (3.5 mL). The vial was fitted with a septum, taken out of the glovebox, and heated to 80 ºC. Aliquots (25 µL) of the reaction were periodically removed and diluted with EtOAc. The reaction was monitored by reverse phase HPLC (70/30 MeCN/H$_2$O containing 1% formic acid). After 2 hours, a 24% yield of **2** was obtained relative to the total [(imam)$_2$Cu](PF$_6$)$_2$ added. After 20 hours, a 42% yield of **2** was obtained relative to the total [(imam)$_2$Cu](PF$_6$)$_2$ added.

Stoichiometric N–N coupling with Cu(OTf)$_2$ as oxidant (eq 4)

A vial with stir bar was charged with Cu(OTf)$_2$ (0.20 mmol), ^{n}Bu$_4$NBr (0.20 mmol or not) and base (if it is a solid) and fitted with a septum. The vial was then vacuumed and refilled with N$_2$ for three times. A solution of imine **3** and 4,4′-difluorobiphenyl in DMF (0.2 mmol of each in 2.0 mL DMF with the latter as internal standard) was added to the vial. Then, base (if it is a liquid) was added into the solution with a syringe. The reaction was stirred for 14 h at room temperature. An aliquot (~0.2 mL) was removed from the reaction, added to NMR tubes and diluted with DMF (0.4 mL). The reaction yield was determined by ^{19}F NMR spectroscopy by integration of **4** relative to an internal standard. The stoichiometry of every component in each reaction and results are shown in Figure S11.

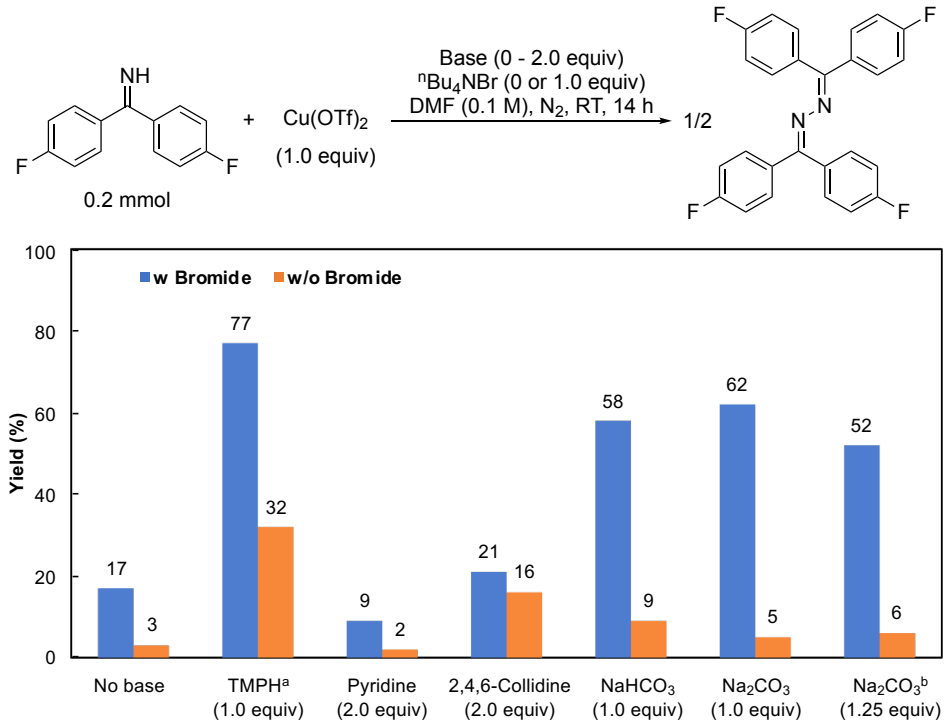

Figure S11. Yields of azine **4** using different bases, with and without bromide. [a]TMPH = 2,2,6,6-Tetramethylpiperidine; [b]Conditions: imine (0.2 mmol), Cu(OTf)$_2$ (1.25 equiv), pyridine (2.5 equiv), Na$_2$CO$_3$ (1.25 equiv) and ^{n}Bu$_4$NBr (1.25 equiv or not) at RT for 3 h.

10. EPR spectra of Cu compounds

Solutions of 10 mM of $CuCl_2$(benzophenoneimine)$_2$ in DMF, and (imam)$_2$Cu(PF_6)$_2$ and (imam)$CuCl_2$ in DMSO, were chilled to a glass in liquid N_2 before insertion into an EPR cavity and further cooled to 15 K in a stream of He. These samples exhibited axial EPR signals for the Cu^{II} species (Figure S12a). The spectrum of $CuCl_2$(benzophenoneimine)$_2$ in DMF is similar to the previously reported spectrum of a similar complex as a powder, suggesting that it dissolves without dissociation of the imine ligands.[7] The large Cu-hyperfine coupling observed in the $g_{||}$ signal does not support a ligand-based radical in the ground state of these complexes. Spectra were also recorded for Cu(OTf)$_2$ in DMF in the presence and absence of 4,4'-difluorobenzophenoneimine and bromide, mimicking the conditions used for stoichiometric coupling of the imine ([Cu^{II}] = 10 mM, [Br^-] = 10 mM, [imine] = 100 mM; cf. Figure S11). In contrast to the data obtained for $CuCl_2$(benzophenoneimine)$_2$, Cu(OTf)$_2$ showed no evidence for binding of the imine. The EPR spectrum revealed ^{14}N superhyperfine coupling (Figure S12b), and identical spectra were obtained in the absence of bromide or imine. These spectra support formation of a Cu^{II}/DMF solvate, similar to that previously studied by X-ray scattering.[8] Addition of 100 mM TMPH significantly changes the signal (Figure S12c), but the spectrum is identical in the presence or absence of imine. These data suggest that TMPH, but not imine, coordinates to Cu^{II} under these conditions.

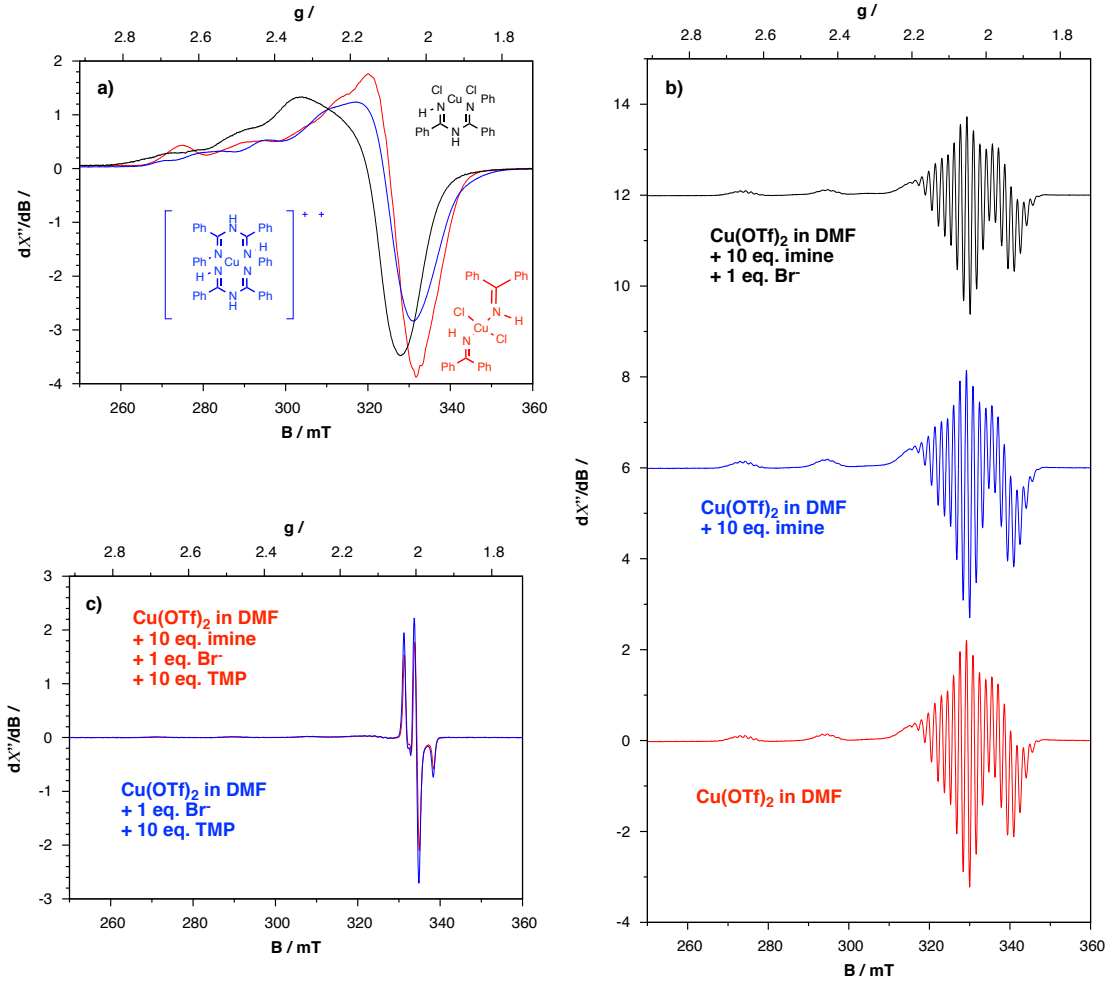

Figure S12. EPR spectra of a) complexes in DMF (red trace) or DMSO (blue, black traces), b) Cu(OTf)$_2$ preferential coordination by DMF, c) formation of Cu(TMPH) complex. Conditions: 9.3 GHz, 15 K.

11. Crystallographic information for $(imam)_2Cu(PF_6)_2 \cdot 2Et_2O$

Data Collection

A purple crystal with approximate dimensions 0.144 x 0.128 x 0.055 mm^3 was selected under oil under ambient conditions and attached to the tip of a MiTeGen MicroMount©. The crystal was mounted in a stream of cold nitrogen at 100(1) K and centered in the X-ray beam by using a video camera.

The crystal evaluation and data collection were performed on a Bruker Quazar SMART APEXII diffractometer with Mo K_α ($\lambda = 0.71073$ Å) radiation and the diffractometer to crystal distance of 4.96 cm.[9]

The initial cell constants were obtained from three series of ω scans at different starting angles. Each series consisted of 12 frames collected at intervals of 0.5º in a 6º range about ω with the exposure time of 3 seconds per frame. The reflections were successfully indexed by an automated indexing routine built in the APEXII program suite. The final cell constants were calculated from a set of 9792 strong reflections from the actual data collection.

The data were collected by using the full sphere data collection routine to survey the reciprocal space to the extent of a full sphere to a resolution of 0.78 Å. A total of 112793 data were harvested by collecting 6 sets of frames with 0.5º scans in ω and φ with exposure times of 10 sec per frame. These highly redundant datasets were corrected for Lorentz and polarization effects. The absorption correction was based on fitting a function to the empirical transmission surface as sampled by multiple equivalent measurements.[10]

Structure Solution and Refinement

The systematic absences in the diffraction data were uniquely consistent for the space group $P2_1/n$ that yielded chemically reasonable and computationally stable results of refinement.[11–16]

A successful solution by the direct methods provided most non-hydrogen atoms from the *E*-map. The remaining non-hydrogen atoms were located in an alternating series of least-squares cycles and difference Fourier maps. All non-hydrogen atoms were refined with anisotropic displacement coefficients except for the minor component disorder atoms, C47a and C48a. Most hydrogen atoms were included in the structure factor calculation at idealized positions and were allowed to ride on the neighboring atoms with relative isotropic displacement coefficients. Atoms H1, H2, H4, and H5 were found in the difference Fourier map and refined independently. Atoms H5 and H2 participate in the N5–H5…O2 and N2–H2…O1 hydrogen-bonding interactions. The D…A distances and D–H…A angles are 2.8325(16) Å /2.8645(16) Å and 166.5(17)°/ 171.5(17)°, respectively.

The asymmetric unit also contained two diethyl ether solvent molecules, one of which had an ethyl that was partially disordered over two positions. The occupancy of the major component was 93.1(4) %. The minor disordered component of the ether was refined with distance restraints. Distal interactions were observed between Cu1 and both F6 and F7. These interactions followed an octahedral motif with distances Cu1–F6 and Cu1–F7 of 2.5369(10) and 2.5258(10) Å and the F6–Cu1–F7 angle of 172.15(3)°. The Cambridge Structural Database contains 25 related structures with similar Cu…PF_6 interactions with an average distance of 2.54(16) Å.

The final least-squares refinement of 670 parameters against 11042 data resulted in residuals *R* (based on F^2 for $I \geq 2\sigma$) and *wR* (based on F^2 for all data) of 0.0275 and 0.0725, respectively. The final difference Fourier map was featureless.

Summary

Crystal Data for $C_{40}H_{34}CuF_{12}N_6P_2 \bullet 2(C_2H_5)_2O$ (M =1100.45 g/mol): monoclinic, space group $P2_1/n$ (no. 14), a = 21.313(6) Å, b = 9.951(3) Å, c = 24.687(6) Å, β = 107.778(11)°, V = 4986(2) $Å^3$, Z = 4, T = 100.0 K, μ(MoKα) = 0.593 mm^{-1}, *Dcalc* = 1.466 g/cm^3, 112793 reflections measured (2.214° ≤ 2Θ ≤ 54.302°), 11042 unique (R_{int} = 0.0384, R_{sigma} = 0.0186) which were used in all calculations. The final R_1 was 0.0275 (I > 2σ(I)) and wR_2 was 0.0725 (all data).

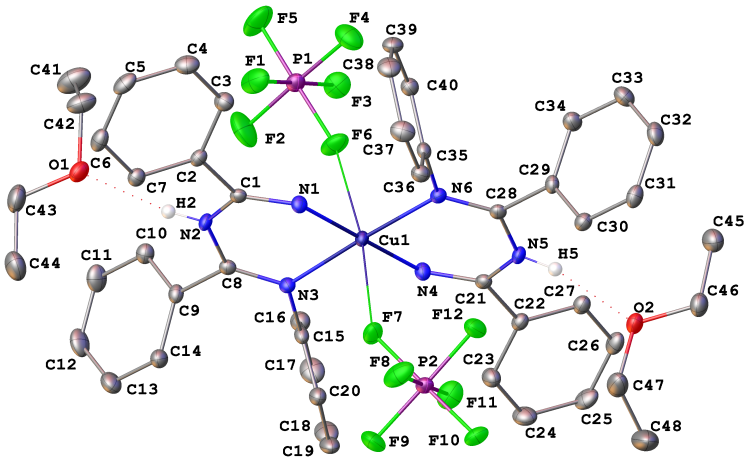

Figure S13. A molecular drawing of the major component of $(imam)_2Cu(PF_6)_2 \cdot 2Et_2O$ shown with 50% probability ellipsoids. All H atoms apart from those involved in the H-bonding network were omitted.

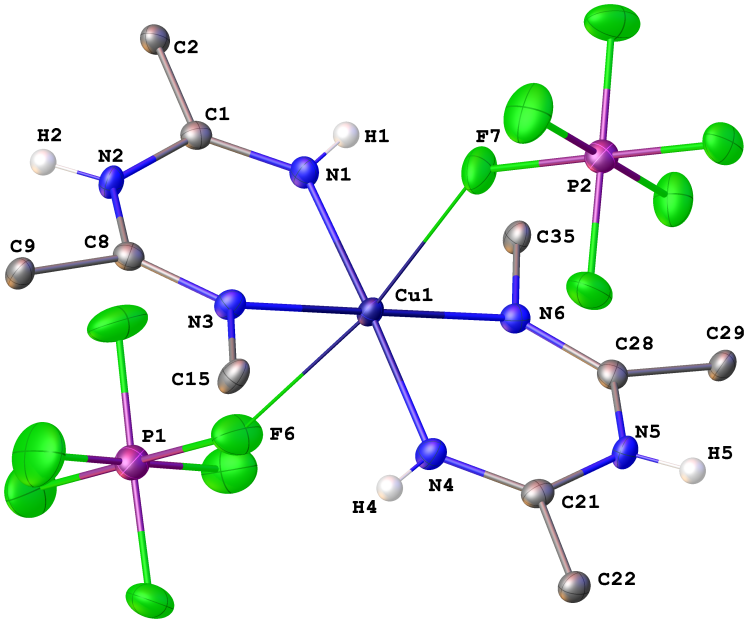

Figure S14. A molecular drawing of copper complex of $(imam)_2Cu(PF_6)_2 \cdot 2Et_2O$ shown with 50% probability ellipsoids. Emphasis is place on the octahedral environment around the central Cu1 atom. Only N bound hydrogens are shown.

Table S5. Crystal data and structure refinement for $(imam)_2Cu(PF_6)_2 \cdot 2Et_2O$.

Empirical formula	$(N_3C_{20}H_{17})_2Cu(PF_6)_2 \bullet 2(C_2H_5)_2O$
Formula weight	1100.45
Temperature/K	100.0
Crystal system	monoclinic
Space group	$P2_1/n$
a/Å	21.313(6)
b/Å	9.951(3)
c/Å	24.687(6)
α/°	90
β/°	107.778(11)
γ/°	90
Volume/Å^3	4986(2)
Z	4
ρ_{calc}g/cm^3	1.466
μ/mm^{-1}	0.593
F(000)	2268.0
Crystal size/mm^3	0.144 × 0.128 × 0.055
Radiation	MoKα (λ = 0.71073)
2Θ range for data collection/°	2.214 to 54.302
Index ranges	$-27 \leq h \leq 27$, $-12 \leq k \leq 12$, $-31 \leq l \leq 31$
Reflections collected	112793
Independent reflections	11042 [R_{int} = 0.0384, R_{sigma} = 0.0186]
Data/restraints/parameters	11042/4/670
Goodness-of-fit on F^2	1.035
Final R indexes [I>=2σ (I)]	R_1 = 0.0275, wR_2 = 0.0698
Final R indexes [all data]	R_1 = 0.0327, wR_2 = 0.0725
Largest diff. peak/hole / e Å^{-3}	0.43/-0.40

12. Spectral Data

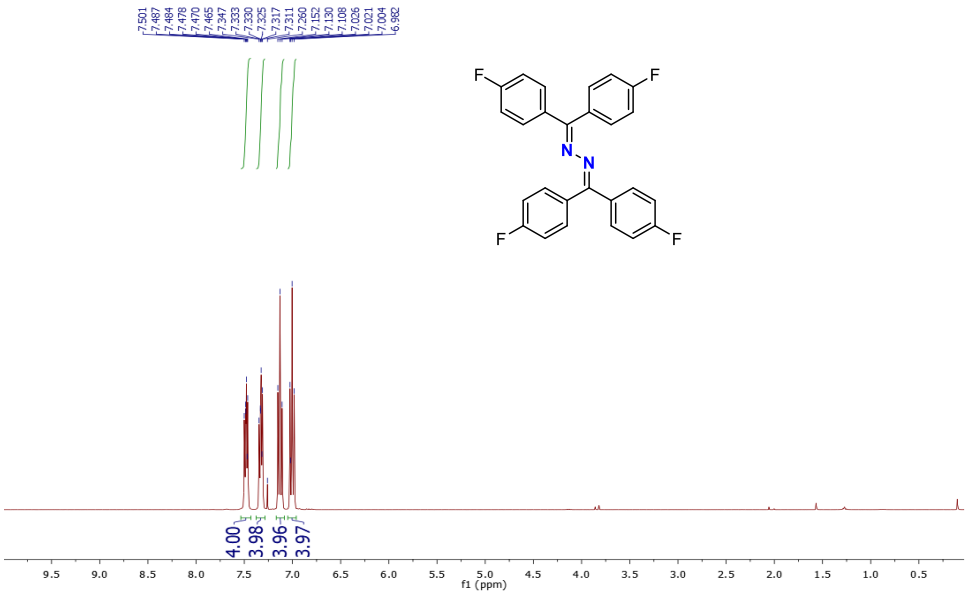

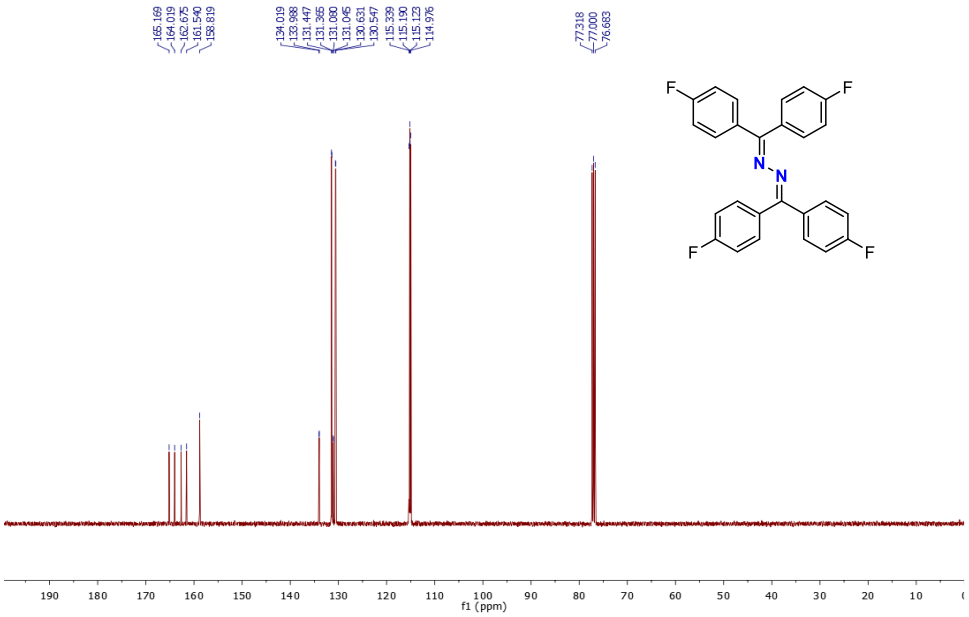

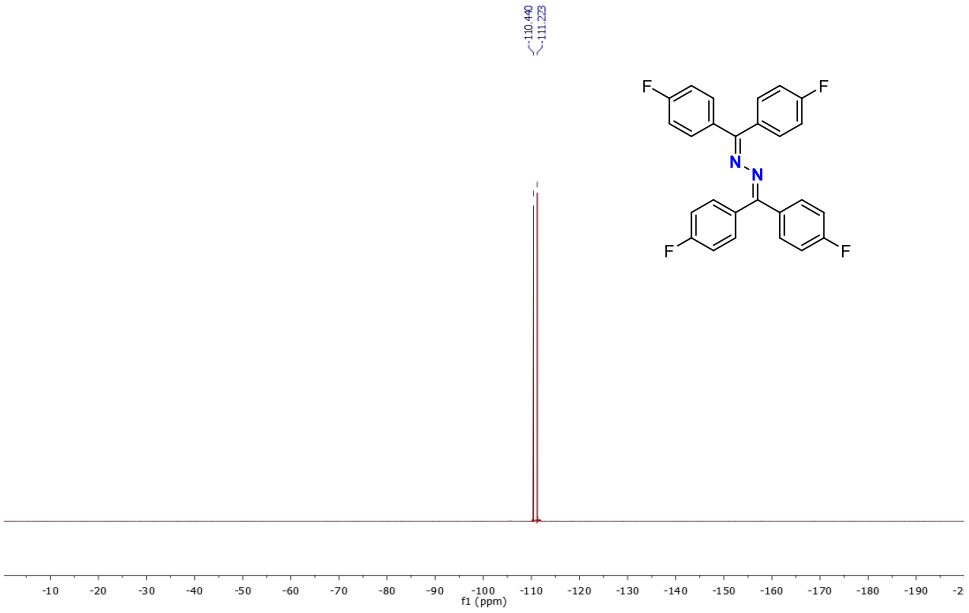

13. References

1. X. Hu, G. Zhang, F. Bu and A. Lei, *Angew. Chem. Int. Ed.* 2018, **57**, 1286–1290.
2. P. M. Osterberg, J. K. Niemeier, C. J. Welch, J. M. Hawkins, J. R. Martinelli, T. E. Johnson, T. W. Root and S. S. Stahl, *Org. Process Res. Dev.* 2015, **19**, 1537–1543.
3. R. Yoshii, A. Hirose, K. Tanaka, Y. Chujo, *J. Am. Chem. Soc.* 2014, **136**, 18131–18139.
4. N. Heße, R. Fröhlich, I. Humelnicu and E.-U. Würthwein, *Eur. J. Inorg. Chem.* 2005, 2189–2197.
5. Nonaqueous potentials and currents are given relative to ferrocene with the IUPAC sign convention: (a) R. G. Bates, *Pure Appl. Chem.* 1976, **45**, 131–134; (b) G. Gritzner and J. Kůta, *Pure Appl. Chem.* 1982, **54**, 1527–1532.
6. I. Noviandri, K. N. Brown, D. S. Fleming, P. T. Gulyas, P. A. Lay, A. F. Masters and L. Phillips, *J. Phys. Chem. B* 1999, **103**, 6713–6722.
7. A. Misono, T. Osa, and S. Koda, *Bull. Chem. Soc. Jpn.* 1968, **41**, 373–377.
8. K. Ozutsumi, S. Ishiguro, and H. Ohtaki, *Bull. Chem. Soc. Jpn.* 1988, **61**, 945–951.
9. Bruker-AXS, APEX3 (Version 2016.5-0), Madison, Wisconsin, USA, 2016.
10. L. Krause, R. Herbst-Irmer, G. M. Sheldrick and D. Stalke, *J Appl Cryst* 2015, **48**, 3–10.
11. G. M. Sheldrick, XPREP (Version 2013/1), Georg-August-Universität Göttingen, Göttingen, Germany, 2013.
12. G. M. Sheldrick, The *SHELX* homepage, http://shelx.uni-ac.gwdg.de/SHELX/, 2013.
13. G. M. Sheldrick, *Acta Cryst A* 2015, **71**, 3–8.
14. G. M. Sheldrick, *Acta Cryst C* 2015, **71**, 3–8.
15. O. V. Dolomanov, L. J. Bourhis, R. J. Gildea, J. a. K. Howard and H. Puschmann, *J Appl Cryst* 2009, **42**, 339–341.
16. I. A. Guzei, Programs *Gn*. University of Wisconsin-Madison, Madison, Wisconsin, USA, 2007-2013.